

## CHAPTER IV

### RESULT AND DISCUSSION

#### 4.1 Characterization of Cellulose Fibers Derived from Banana Trunks

##### 4.1.1 Raw Banana Fibers

The SEM image of raw banana fibers, which was prepared from inner core of banana trunk, illustrates that the raw banana fiber exhibited long and slender microfibril structure, and the individual or aggregated fragments can be seen as shown in Figure 4.1. The width and length were estimated from the selected SEM images. The average length and diameter of the raw banana fibers were found to be 12.56 mm and 1.85 mm, respectively, corresponding to the aspect ratio (L/D) of about 6.79.

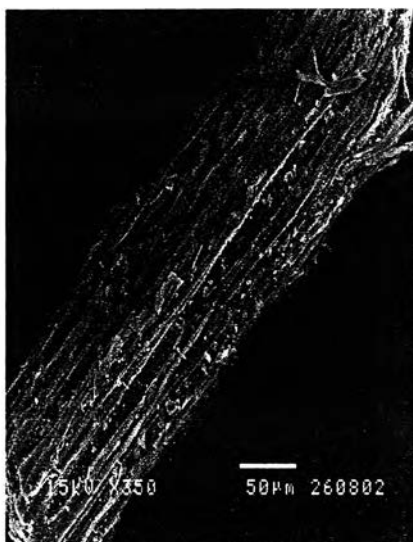


**Figure 4.1** SEM image of raw banana fibers obtained from inner core of banana trunks.

##### 4.1.2 Preparation of Cellulose Sheets

###### 4.1.2.1 *Effect of NaOH concentrations for prepare cellulose sheets*

*(HCl concentration was fixed at 2 M)*

#### 4.1.2.1.1 Morphology Analysis

The SEM images reveal that surface morphology and texture of cellulose sheets had almost no change when NaOH concentration was increased as show in the figure 4.2.

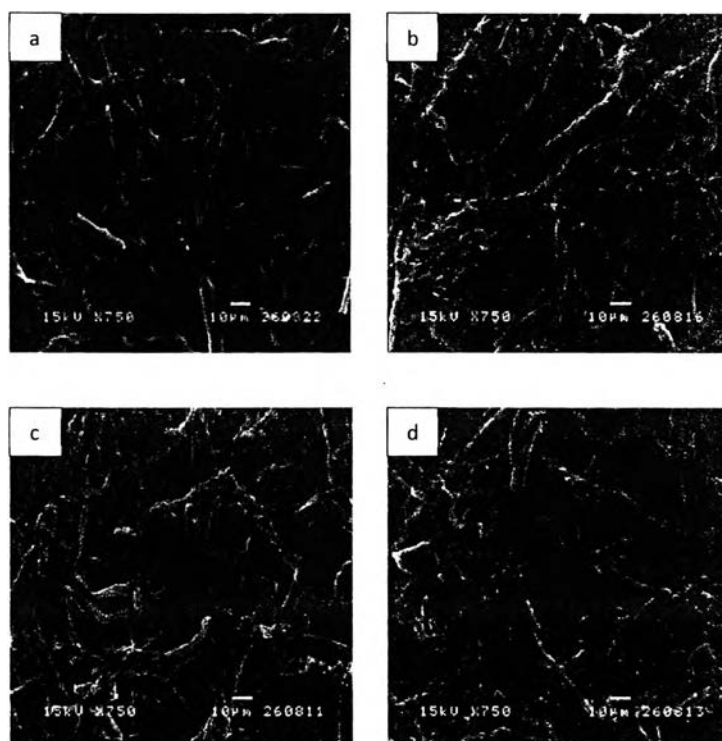


**Figure 4.2** SEM images of cellulose sheets at NaOH concentrations a) 5% w/v, b) 10% w/v, c) 15% w/v and d) 20% w/v.

#### 4.1.2.1.2 Chemical Analysis

The chemical structures of the raw banana fibers and the treated cellulose fibers were investigated with using FTIR spectroscopy. Figure 4.3, FTIR spectrum of the treated cellulose fibers had similar pattern among the studied the NaOH concentrations. The raw banana fibers and treated cellulose fibers show a broad band of the OH-stretching in a wavenumber  $3600\text{ cm}^{-1}$  to  $3000\text{ cm}^{-1}$ . The peak at  $1731\text{ cm}^{-1}$  disappeared after treatment due to removed of acetyl and uronic ester groups of the hemicellulose or the ester linkage of carboxylic group of the ferulic and p-coumeric acids of lignin and/ or hemicellulose (Elanthikkal *et al.*,

2010). The peak at  $1621\text{ cm}^{-1}$  decreased after treatment represented to eliminate the aromatic C=C of lignin. Other two peaks at  $1022$  and  $893\text{ cm}^{-1}$  increased after treatment. These peaks represented to -C-O-C- pyranose ring and  $\beta$ -glycosidic linkages of cellulose, respectively.

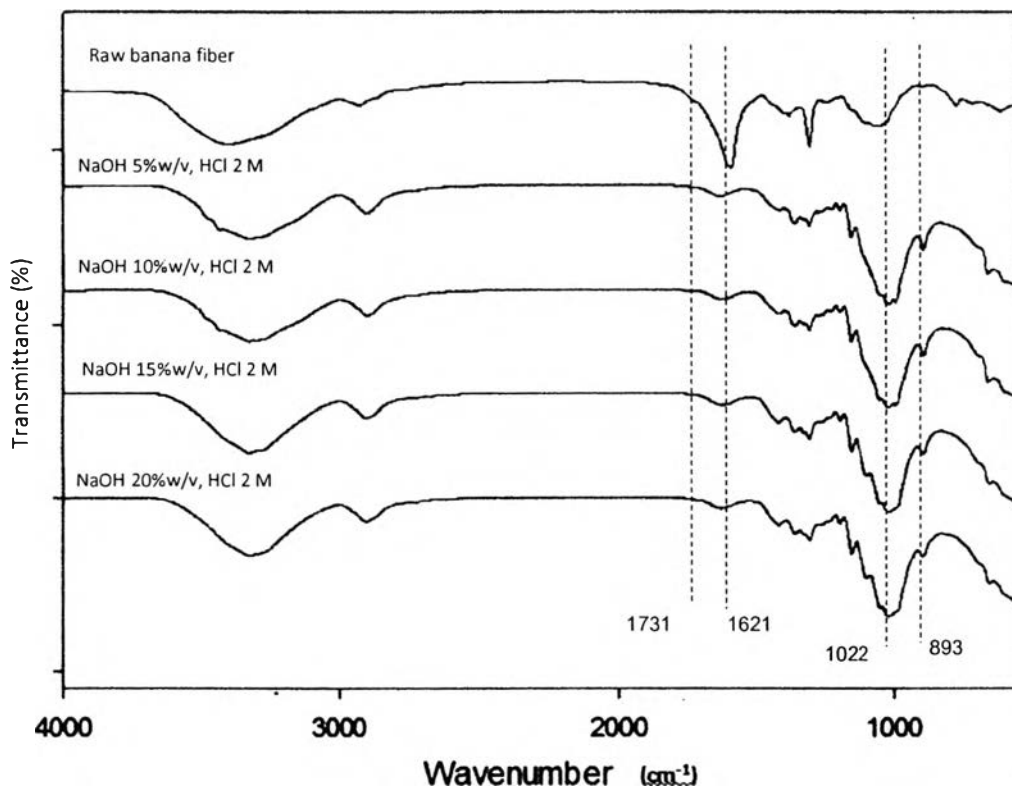


**Figure 4.3** FTIR spectra of banana fibers before and after treatment.

#### 4.1.2.1.3 Crystallinity Analysis

In Figure 4.4, it can be seen that the alkali- and acid-treated cellulose fibers show the characteristic peaks with higher intensities than the raw banana fibers. XRD diffractograms showed four diffraction peaks at  $2\theta$  of  $12.5^\circ$ ,  $16.5^\circ$ ,  $22.6^\circ$  and  $34.7^\circ$  which refer to the 110, 110, 002 and 004 diffraction planes, respectively (Maheswari *et al.*, 2012). The peak at  $12.5^\circ$  in cellulose treated with NaOH 5% w/v cannot be observed, seen only peak at  $16.5^\circ$  due to the large amount of the remaining hemicellulose and lignin content (Vieira *et al.*, 2011). However, at NaOH 15% w/v the peak  $12.5^\circ$  can be clearly observed and the similar thing was

observed at 20% NaOH. Therefore, 15% NaOH was used for the treatment of cellulose fiber.

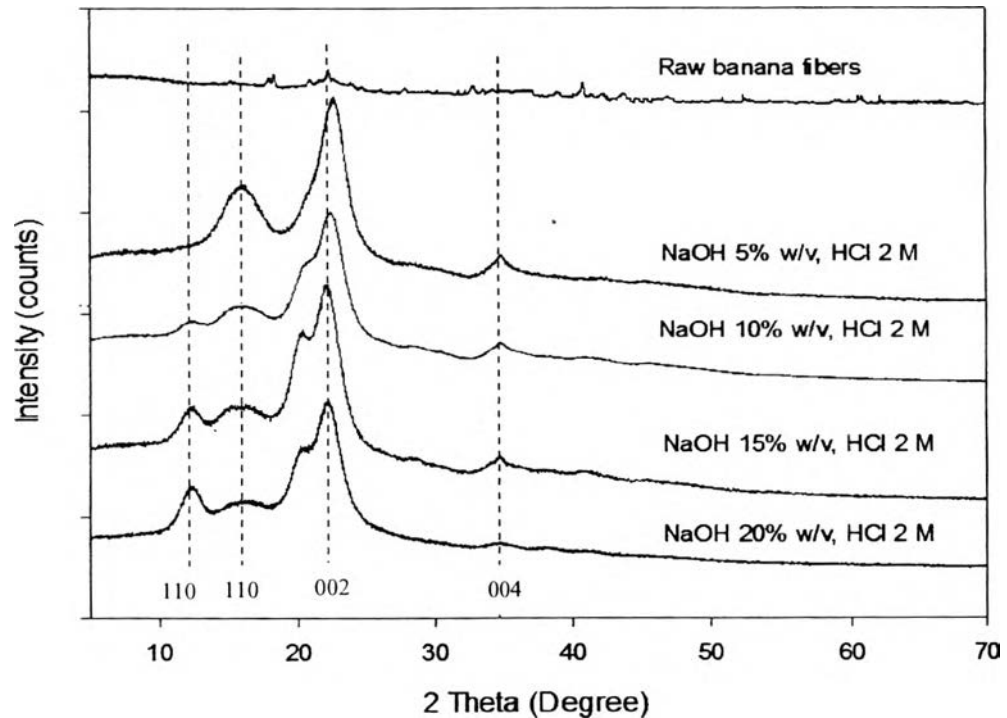


**Figure 4.4** XRD curves of banana fibers before and after treatment.

#### 4.1.2.2 Effect of HCl Concentrations for Prepare Cellulose Sheets (NaOH concentration was fixed at 15 %w/v)

##### 4.1.2.2.1 Morphology Analysis

From figure 4.5, the SEM images reveal that the more HCl concentrations increase, the more cellulose fibers length decrease. Due to a loss of fibrous character identity occurs, indicating the surface etching and erosion by hydrolysis process (Elanthikkal *et al.*, 2010).

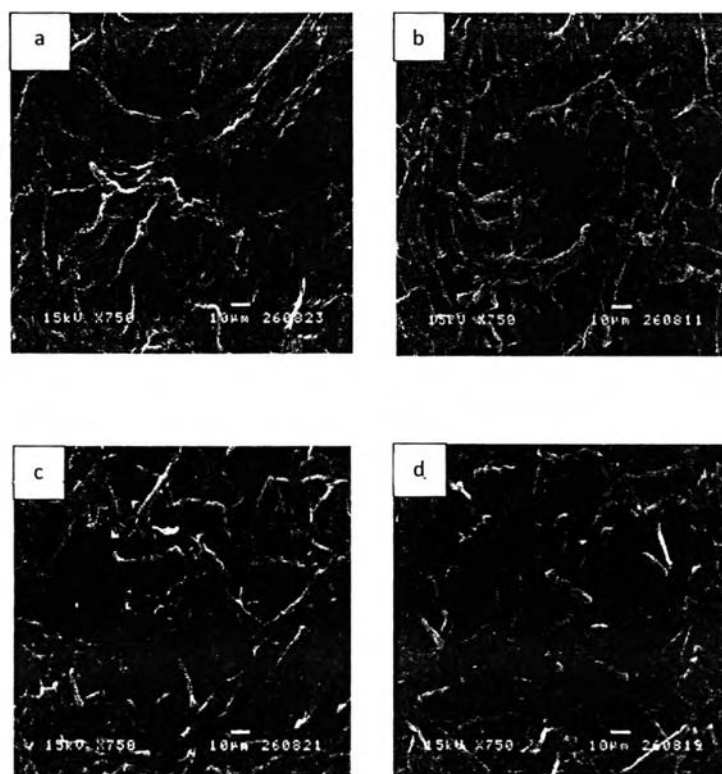


**Figure 4.5** SEM images of cellulose sheets at HCl concentrations a) 1.5 M, b) 2 M, c) 2.5 M and d) 3 M.

#### *4.1.2.2.2 Chemical Analysis*

The FTIR spectra as shown in Figure 4.6 at every HCl concentrations had similar result as previously described in vary NaOH concentrations.

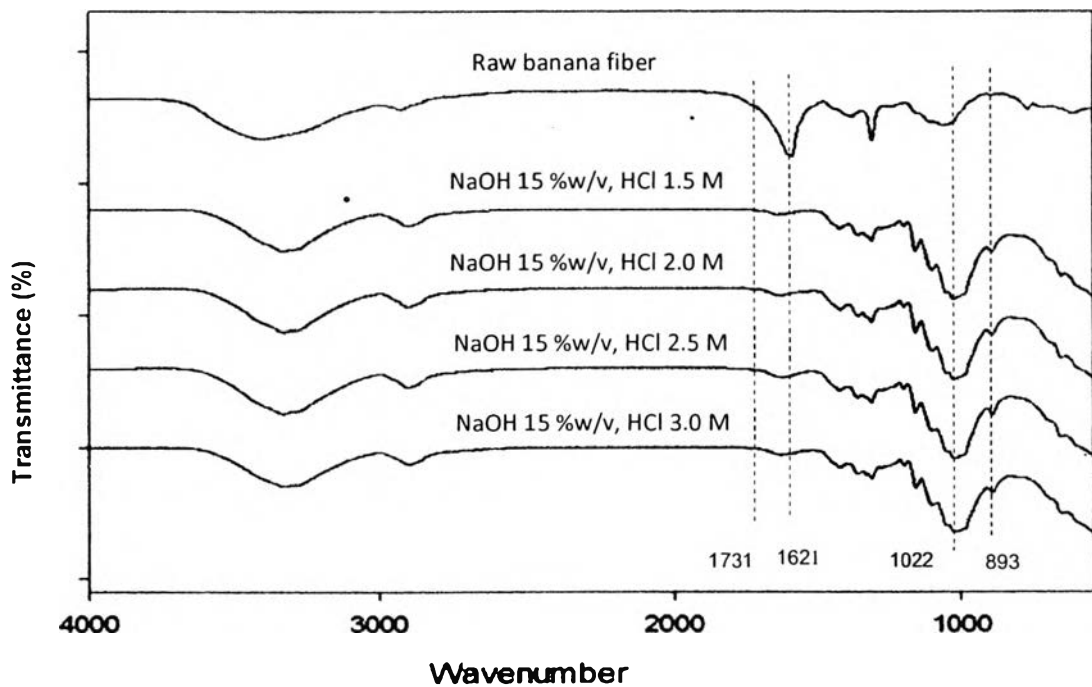


**Figure 4.6** FTIR spectra of banana fibers before and after treatment.

#### 4.1.2.2.3 Crystallinity Analysis

In Figure 4.7, indicated that after treating the raw banana fibers can provided more clearly peak than the raw banana fibers. The peak appeared at  $2\theta$  of  $12.5^\circ$ ,  $16.5^\circ$ ,  $22.6^\circ$  and  $34.7^\circ$  which refer to the 110, 110, 002 and 004 diffraction planes, respectively (Maheswari *et al.*, 2012) in which similar to using vary NaOH concentrations. The clearly peak is due to elimination of hemicelluloses and lignin from chemical treatment. The XRD pattern of raw banana fibers that treated with 2.5 M HCl provided more clearly peak than treated with 1.5 and 2 M HCl. After treated with 2.5 M HCl the XRD pattern nothing change.

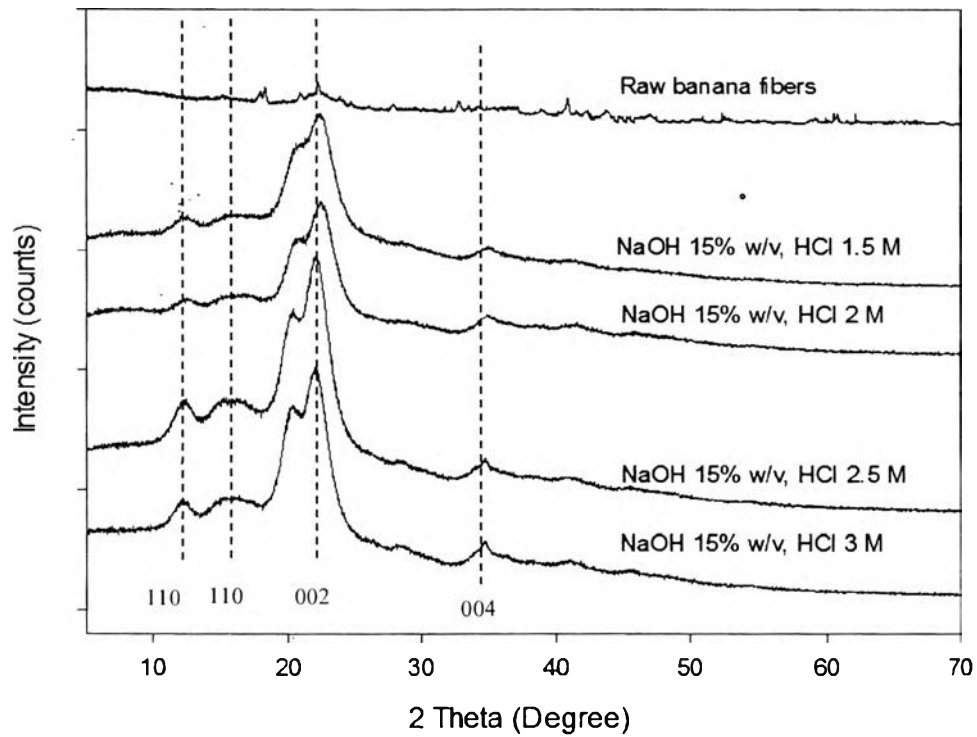


**Figure 4.7** XRD curves of banana fibers before and after treatment.

Therefore, 15% w/v NaOH and 2.5 M HCl was used for prepare cellulose sheets from raw banana fibers in this study. The banana fibers after treated has smoother surface than raw banana fibers as show in Figure 4.8 because removal of hemicellulose and lignin by chemical treatment (Maheswari *et al.*, 2012). It was found that they have average length and diameter 0.42 mm and 3.28  $\mu\text{m}$ , respectively, corresponding to the aspect ratio (L/D) about 128. The treated cellulose fibers have higher aspect ratio than the raw banana fibers, it means that the treated cellulose fibers have higher strength and greater flexibility than the raw banana fibers. The production yield of treated cellulose fibers is 13.12 % as shown in table 4.1.

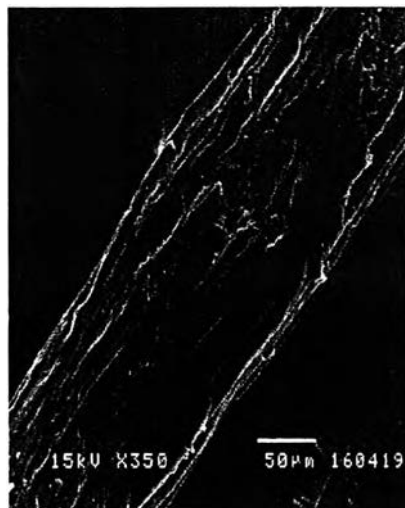


**Figure 4.8** SEM image of treated banana fibers.

**Table 4.1** The production yield of treated cellulose fibers.

Material/ Process	Dry Weight (g)
Inner core of banana trunk	100
Immersed in 15% (w/v) NaOH	30.25
Bleached fiber	20.85
HCl 2.5 M hydrolyzed cellulose fiber	13.12

The thermal degradation behavior of the raw banana fibers, and the treated cellulose fibers were analysed by thermogravimetric analysis in  $N_2$  at heating rate of  $10^\circ C/min$ . The TGA of raw banana fibers showed in figure 4.9 the weight loss in four stages. The first stage ranged between  $70^\circ C$  and  $140^\circ C$  that might correspond to the remove of adsorbed water. The second stage of the weight loss started at  $200^\circ C$



to 308°C is due to the degradation of hemicellulose. Thermal decomposition of cellulose started at about 308°C followed by two major losses of weight during the decomposition of lignin. In comparison with treated banana fibers, the cellulose fibers which derived from banana trunks, the graph showed the weight loss in three stages. The first region in the temperature regime of 50-150°C is due to the evaporation of water. The second transition region at around 200-308°C is due to degradation of residual hemicellulose. The third stage of weight loss is occurred about 308°C, is due to the decomposition of cellulose. The results indicated that hemicellulose and lignin were removed from raw banana fibers after the treatment of alkali and acid.

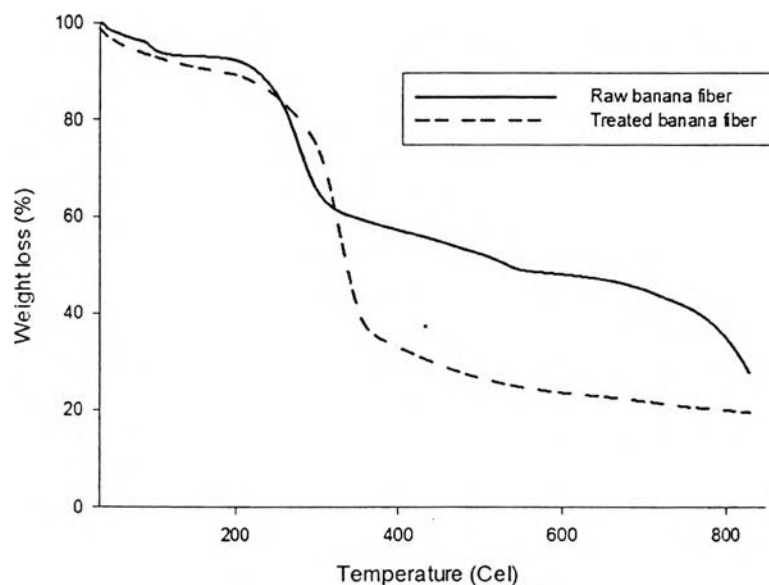


**Figure 4.9** The thermogravimetric analysis of raw banana fibers and cellulose fibers.

## 4.2 Characterization of Cellulose Fibers Treated with Solution Plasma by Study the Effect of Plasma Treatment Time

### 4.2.1 Effect of Solution Plasma Treatment on Appearance

Figure 4.10 shows the appearance of cellulose treated with solution plasma by vary plasma treatment time and then make them into the sheet forms. The

average thickness is  $0.089 \pm 0.011$  millimeter. When the plasma treatment time increased, the surface of cellulose sheet appeared black spots. It may be due to the degradation of cellulose when plasma treatment time increased, some parts of cellulose burned with plasma. Therefore, the cellulose sheets treated with solution plasma at 180 and 240 minutes were not considered in the next part because they have a lot of black spots on the surface.

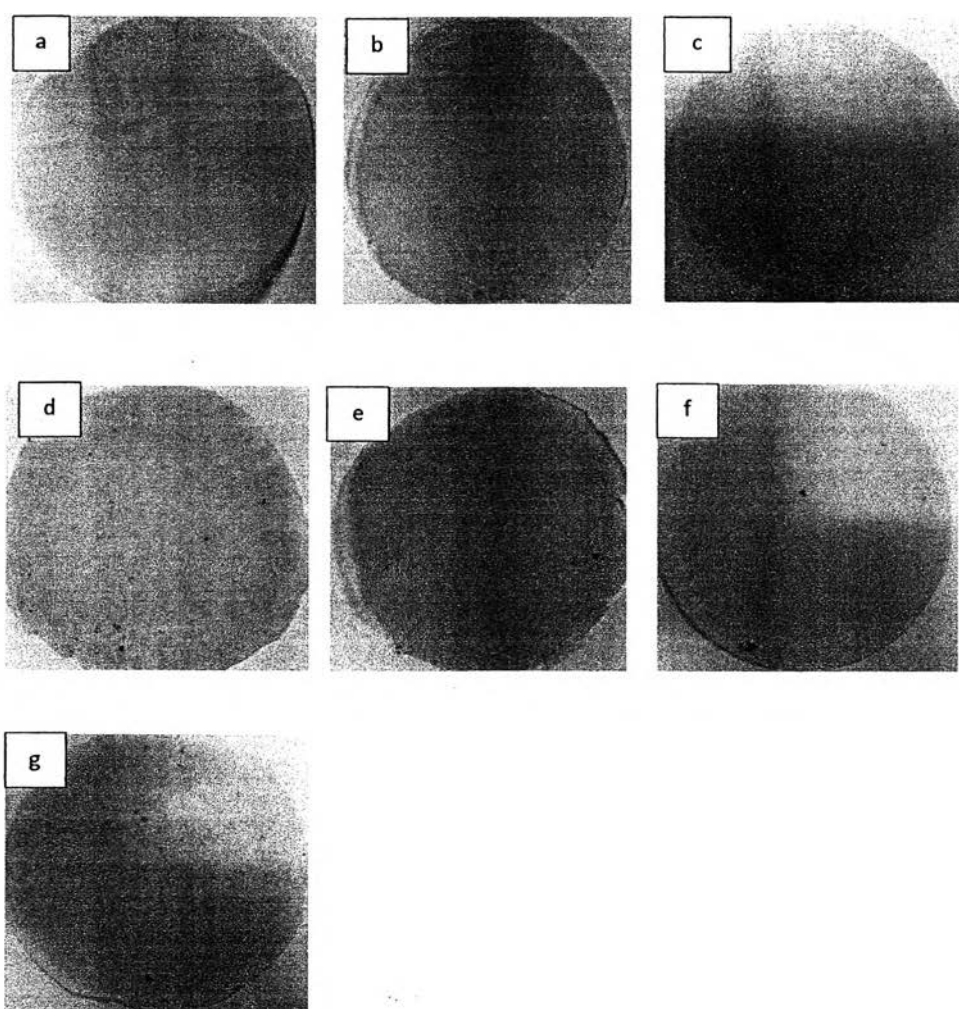


**Figure 4.10** Appearance of cellulose sheets at plasma treatment time (a) 0, (b) 30, (c) 60, (d) 90, (e) 120, (f) 180 and (g) 240 minutes.

#### 4.2.2 Effect of Solution Plasma Treatment on Morphology Analysis

The solution plasma treat on cellulose at any different plasma treatment time was not effect to surface of cellulose sheets. Some fibers form continuous surface with some large fibers has been observed on the surface.

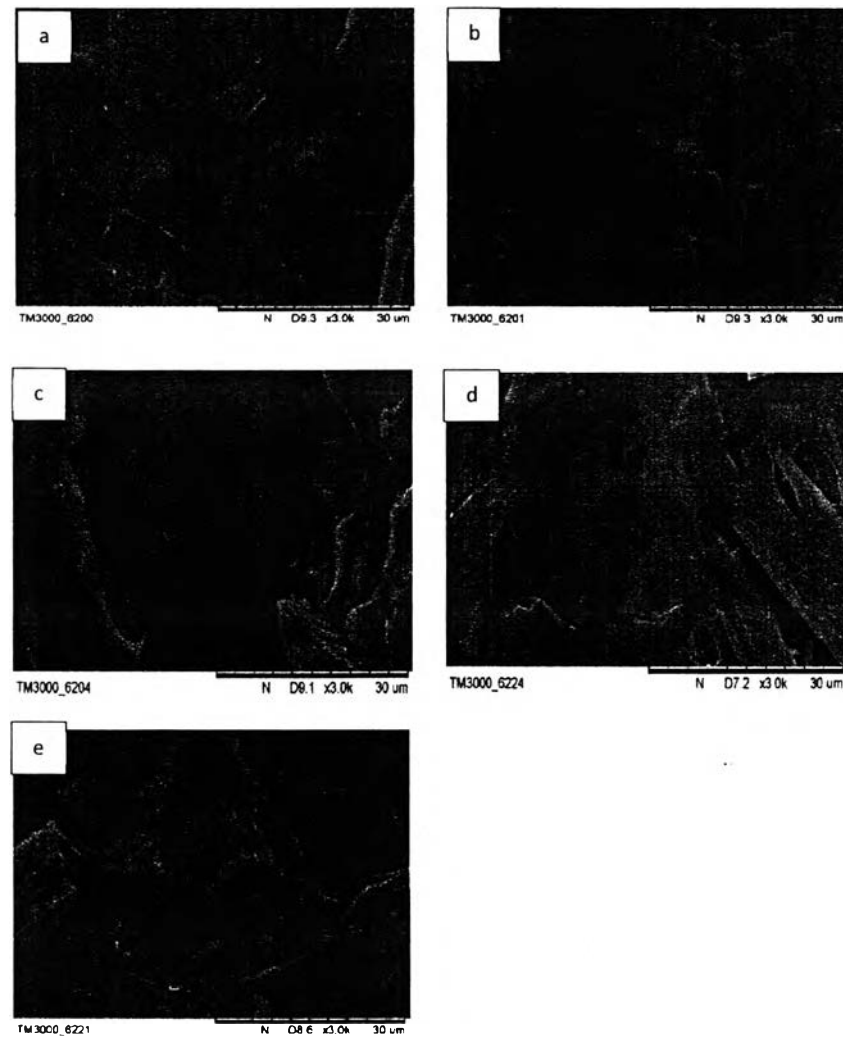


**Figure 4.11** SEM image of cellulose sheets at plasma treatment time (a) 0, (b) 30, (c) 60, (d) 90, (e) 120 minutes.

#### 4.2.3 Effect of Solution Plasma Treatment on Water Contact Angle Analysis

The hydrophilic properties of cellulose treated with solution plasma by using the different plasma treatment time were characterized by water contact angle measurement. Figure 4.12 shows the effect of solution plasma treatment on the water

contact angle on the surface of cellulose sheet. The water contact angle slowly decreased from 65.9°, 60.2°, 57.5°, 55.4° to 53.2° with plasma treatment time 0, 30, 60, 90 and 120 minutes, respectively. After plasma treatment time 60 minutes the water contact angle value slowly decreased as seen from the figure 4.13.

The result indicated that solution plasma leading to an increase in the hydrophilic property of cellulose sheet. This should be due to the solution plasma can generate a new functional group to the cellulose.

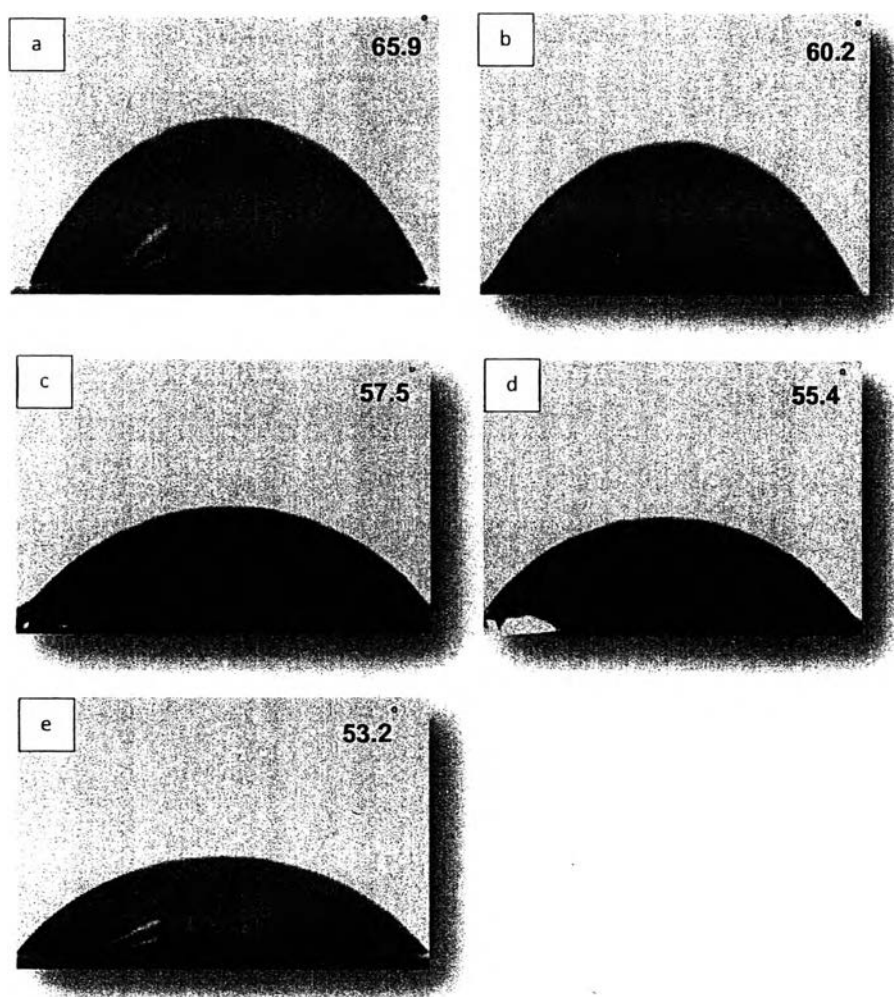


**Figure 4.12** Interfacial water contact angle of cellulose sheets treated with solution plasma (a) 0, (b) 30, (c) 60, (d) 90 and (e) 120 minutes.

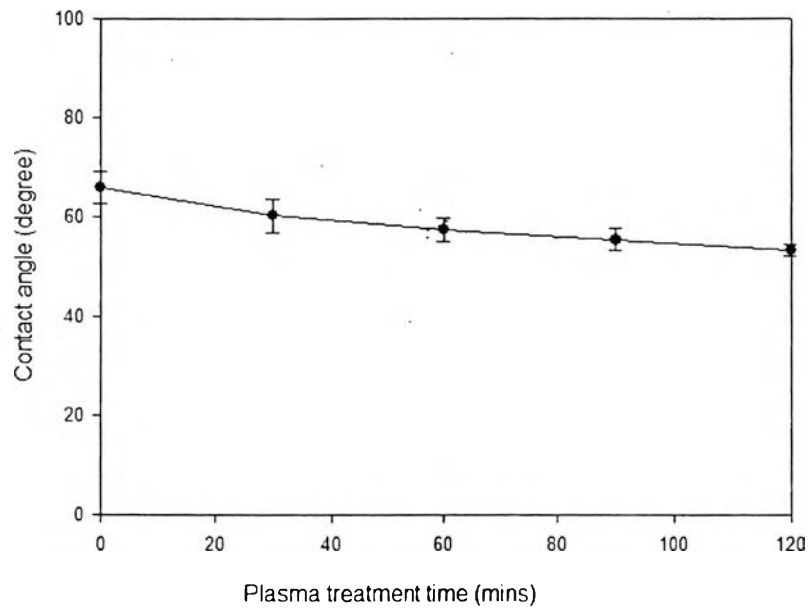


**Figure 4.13** Effect of plasma treatment time on water contact angle on cellulose sheets.

#### 4.2.4 Effect of Solution Plasma Treatment on Bending Testing

The stiffness of cellulose sheets treated with solution plasma from increased with increasing plasma treatment time. But after plasma treatment time longer than 60 minutes, the stiffness slightly increased as showed in Figure 4.14. It may be caused by the interaction between the cellulose in plasma process but after plasma treatment time longer than 60 minutes some cellulose fibers degraded by plasma treatment, so the stiffness slightly increased. That agreed with the appearance of cellulose sheet when increase plasma treatment time.

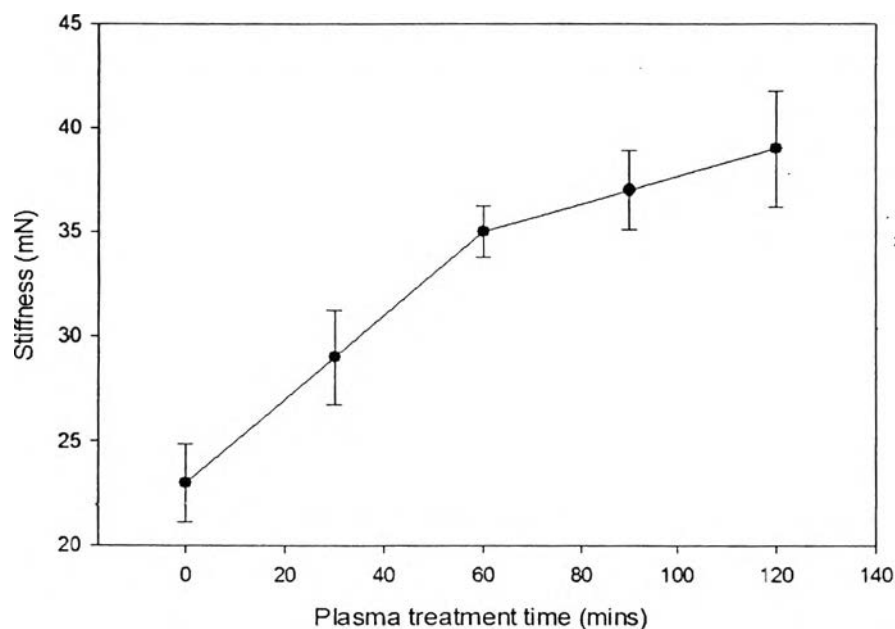


**Figure 4.14** Effect of plasma treatment time on bending testing of cellulose sheets.

#### 4.2.5 Effect of Solution Plasma Treatment on Chemical Composition

The chemical composition of solution plasma-treated cellulose sheet was investigated by using the FTIR technique. The FTIR spectra of the cellulose sheets before and after the solution plasma treatment was determined as showed in Figure 4.15. After the solution plasma treatment, the peak at  $1708\text{ cm}^{-1}$  increased in intensity corresponding to C=O stretching vibration (Ragojanu *et al.*, 2010). The intensity of the peaks was increase with increasing the solution plasma treatment time, implying a higher amount of the new oxygen-containing functional groups (C-O, C=O and O-C=O) at a longer plasma treatment time.

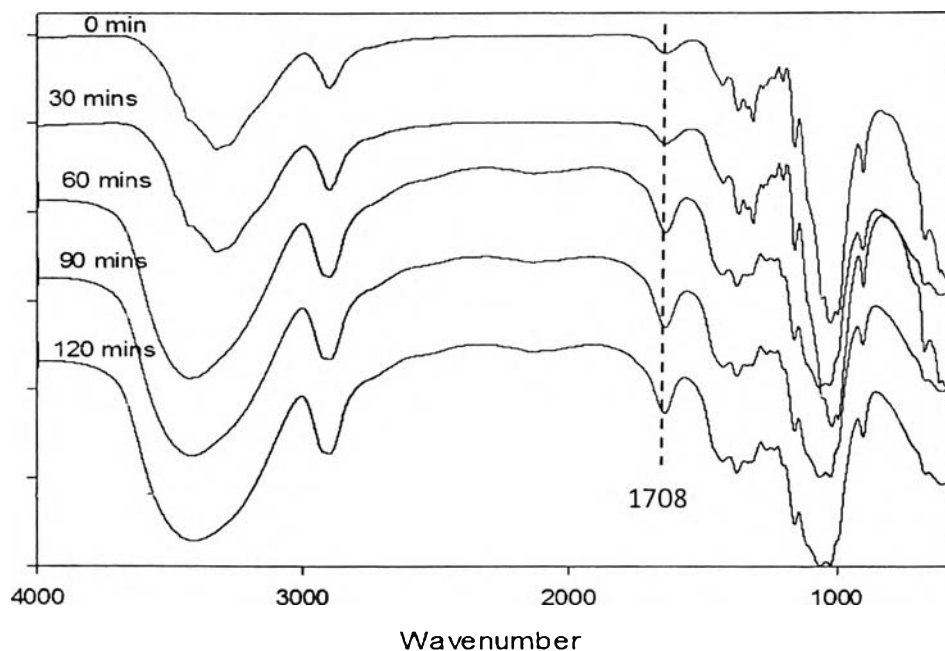


**Figure 4.15** FTIR spectra of cellulose sheets at different solution plasma treatment time.

Moreover, the chemical composition of treated-cellulose sheets was further examined by using the XPS technique. Figures 4.16 (a), (b), (c), (d) and (e) showed the C (1s) spectra of untreated cellulose sheets and plasma-treated cellulose sheets at 0, 30, 60, 90 and 120 minutes, respectively. The result showed that the chemical composition of untreated cellulose sheets is altered after the plasma treatment which can be observed from three main peaks. The peak at 285.0, 286.5 and 288.0 eV was attributed to C-C/C-H, C-OH and C-O-C/C=O bond (Rjeb *et al.*, 2004). The last peak at 288.8 eV was attributed to O-C=O bond (Morent *et al.*, 20107). As showed in table 4.2, the percentage of oxygen-containing polar group which are C-OH, C-O-C/C=O and O-C=O are increased as increasing the plasma treatment time whereas the percentage of C-C/C-H was decreased. It might be implied that the solution plasma changed the chemistry of cellulose sheets by decomposition of polymer chains and oxidation reactions forming aldehyde and carboxylic acid/carboxylate groups lead to the formation of the oxygen-containing polar functional groups, relating to an increase in the C-O-C/C=O and O-C=O bond (Calvimontes *et al.*, 2011). These results were in agreement with the FTIR results.

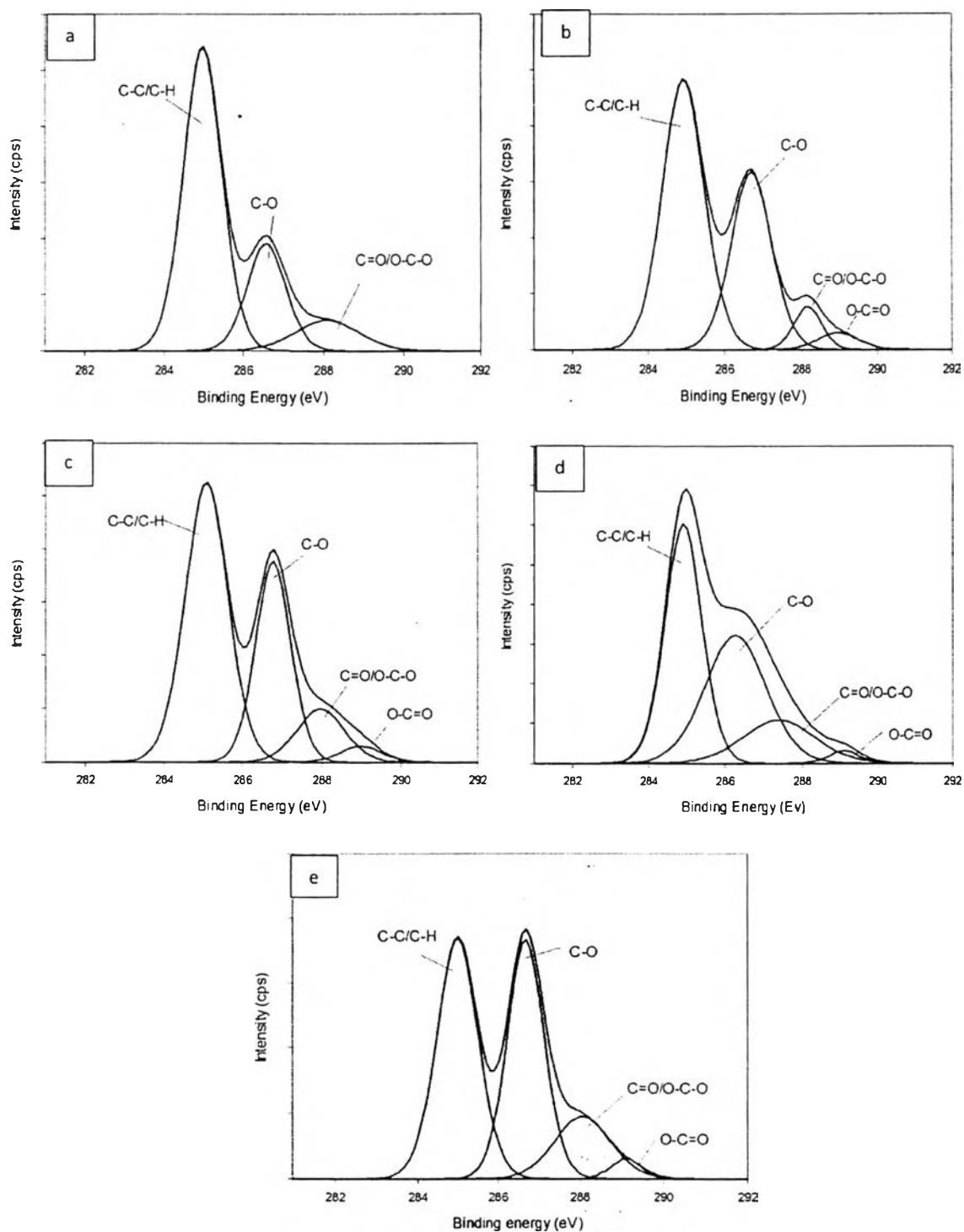


**Figure 4.16** XPS spectra of (a) untreated- cellulose sheet, (b) 30, (c) 60, (d) 90 and (e) 120 minutes plasma-treated cellulose sheets, respectively.



**Table 4.2** Effect of plasma treatment time on the percentage of chemical compositions.

Treatment time (mins)	Percentage of chemical composition			
	285.0 eV C-C/C-H	286.5 eV C-O	288.0 eV C-O-C/C=O	288.8 eV O-C=O
0	68.9	23.3	7.8	-
30	60.1	28.2	9.2	2.5
60	52.5	31.5	12.8	3.2
90	45.8	37.8	13.1	3.3
120	44.2	38.2	14.0	3.6

#### 4.2.6 Effect of Solution Plasma Treatment on Crystallinity

Wide-angle x-ray diffraction (WAXD) patterns were used to study the crystalline structure of cellulose sheet that treated with solution plasma. The characteristic diffractions of untreated, 30, 60, 90 and 120 minutes solution plasma-treated cellulose sheets were showed in Figure 4.17. All of the samples appeared the peak at  $2\theta$  of  $12.5^\circ$ ,  $16.5^\circ$ ,  $22.6^\circ$  and  $34.7^\circ$  which refer to the 110, 110, 002 and 004 diffraction planes, respectively (Maheswari et al., 2012). The result indicated that the treatment with solution plasma does not change the crystallinity of cellulose sheet (Calvimontes *et al.*, 2011).

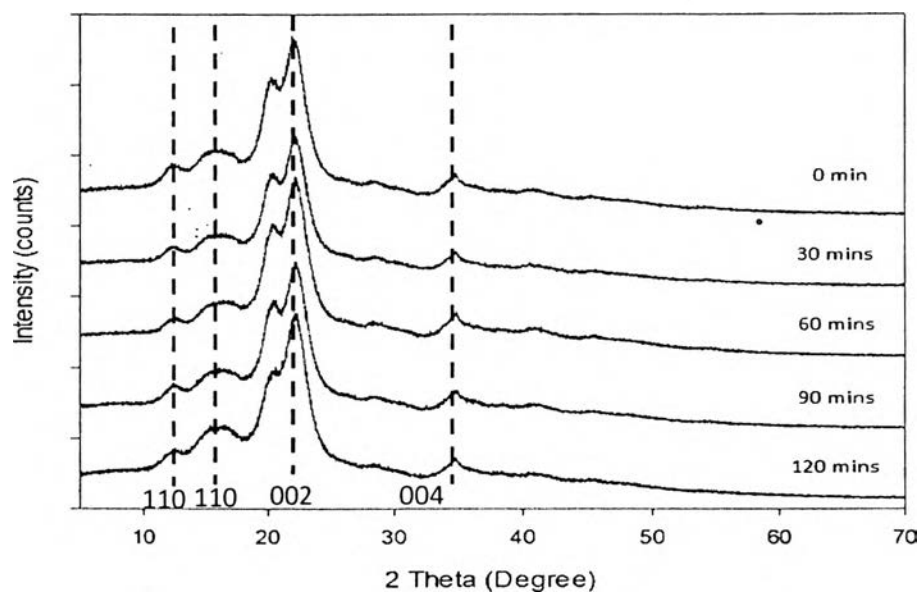


**Figure 4.17** XRD pattern of untreated and solution plasma treated cellulose sheets.

The results from the water contact angle analysis, bending testing, fourier transform infrared spectroscopy (FTIR) and x-ray photoelectron spectroscopy (XPS) indicated that cellulose sheet treated with solution plasma treatment time 60 minutes was enough for treated the cellulose fibers.

### 4.3 Characterization of Polyaniline Coated on Plasma Treated Cellulose Sheets by Using Different Cellulose to Aniline Monomer Ratios

#### 4.3.1 Finding Percent Yield of Polyaniline

The amount of polyaniline that coated on the surface of cellulose sheet can separately determine by did everything the same as prepared polyaniline coated on cellulose sheet by solution plasma except added cellulose fibers. The reactions time was 20 minutes. The %yield can calculated from

$$\% \text{Yield} = \frac{\text{Weight of polyaniline}}{\text{Weight of aniline monomer}} \times 100$$

From the result in the table 4.3 showed that %yield of polyaniline increased with increasing the aniline monomer. However, when used aniline monomer 6g, %yield decreased may be due to amount of hydrochloric acid and ammonium persulfate was not enough for occurring polyaniline.

**Table 4.3** %Yield of polyaniline obtained from different aniline monomer.

Aniline monomer (g)	Polyaniline (g)	%yield
0.5	0.0186	3.7
1	0.0441	4.4
5	0.5007	10.0
6	0.5138	8.6

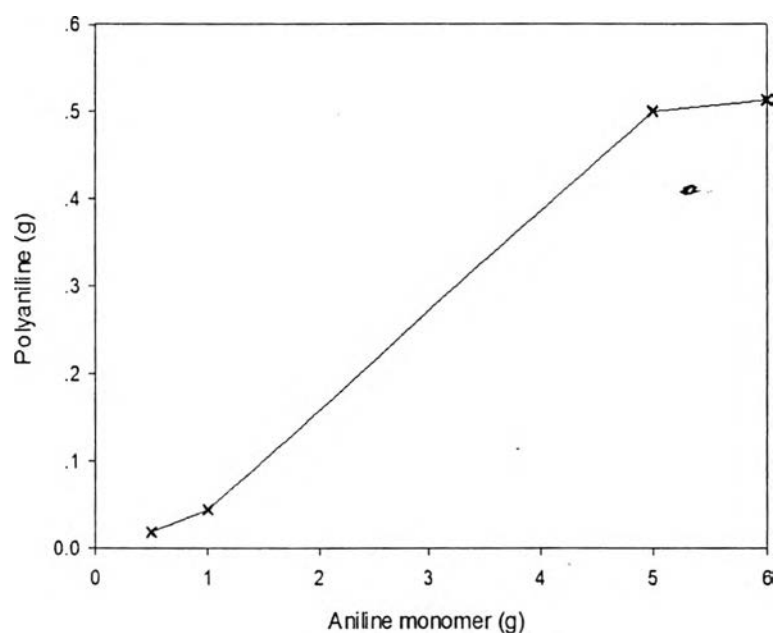


**Figure 4.18** Amount of polyaniline obtained from different amount of aniline monomer.

#### 4.3.2 Compare %Yield of Polyaniline from Conventional Method and Solution Plasma Method

At reaction time 20 minutes, temperature 45 °C solution plasma can provided %yield 10.0 and conventional method can provided %yield 0.072. Therefore, amount of polyaniline from solution plasma had higher %yield than conventional method.

**Table 4.4** %Yield of polyaniline obtained from conventional method and solution plasma method.

Synthesis method	Aniline monomer (g)	Polyaniline (g)	%Yield
Solution plasma	5	0.5007	10.0
Conventional method	5	0.0036	0.072

#### 4.3.3 Compare %Yield of Polyaniline by Using Difference Plasma Treatment Time

The results from table 4.5 showed that the increasing of plasma treatment time from 20, 40 to 60 minutes can provided polyaniline 0.5007, 0.5268 and 0.5311 g, respectively. Therefore, it can conclude that the plasma treatment time longer than 20 minutes less effect on amount of polyaniline.

**Table 4.5** %Yield of polyaniline by using difference plasma treatment time.

Time (minutes)	Aniline monomer (g)	Polyaniline (g)	%Yield
20	5	0.5007	10.0
40	5	0.5268	10.5
60	5	0.5311	10.6

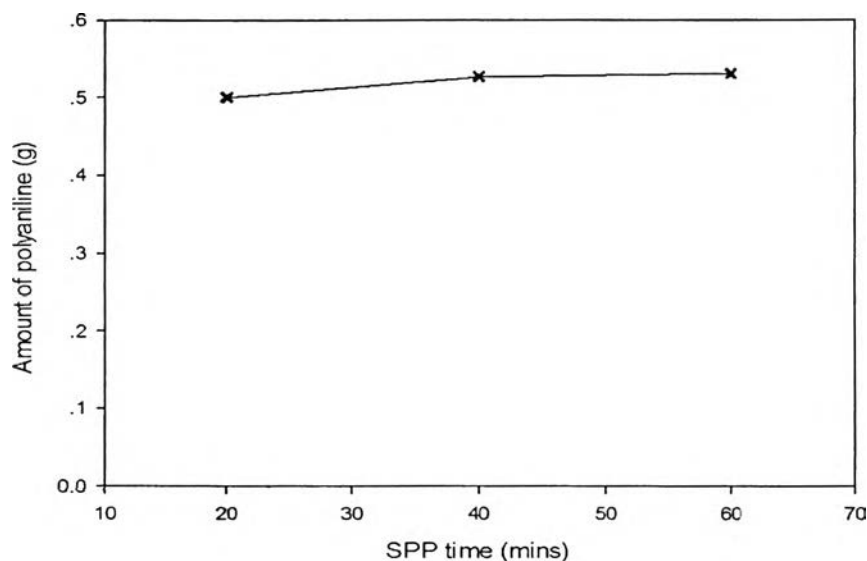


**Figure 4.19** Amount of polyaniline obtained from different plasma treatment time.

Thus, the condition for coating polyaniline on cellulose sheets was used cellulose fibers to aniline monomer ratio 1:5 and solution plasma treatment time 20 minutes.

#### 4.3.4 Compare Electrical Conductivity of Polyaniline Coated on Cellulose Sheet by Solution Plasma Process and Oxidative Polymerization

Polyaniline coated on cellulose sheet by solution plasma process 20 minutes can change the appearance of cellulose sheet from white to dark green but oxidative polymerization 20 minutes cannot change the appearance of cellulose sheet from white to dark green as shown in figure 4.20. The less time that can change cellulose sheet from white to dark green by oxidative polymerization is 60 minutes. Therefore, the comparison electrical conductivity of polyaniline coated on cellulose sheet was selected at solution plasma 20 minutes and oxidative polymerization is 60 minutes. The electrical conductivity of polyaniline coated on cellulose sheet by using solution plasma 20 minutes is  $7.42 \times 10^{-4}$  S/cm and electrical conductivity of polyaniline coated on cellulose sheet by using oxidative polymerization 60 minutes is  $6.99 \times 10^{-4}$  S/cm. The electrical conductivity of two methods was not significantly different.

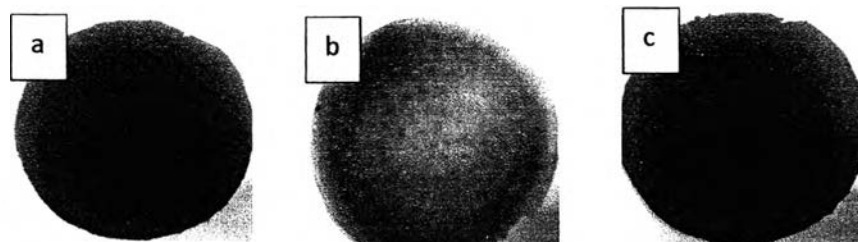


**Figure 4.20** Polyaniline coated on cellulose sheet by a) solution plasma process 20 minutes, b) oxidative polymerization 20 minutes and c) oxidative polymerization 60 minutes.

#### 4.3.5 Compare the Deposition Capacity of Polyaniline Coated on Cellulose Sheet by Solution Plasma Process and Oxidative Polymerization

The deposition capacity of polyaniline coated on cellulose sheet was determined by using ultrasonic bath 30 minutes in distilled water. It found that the sediment of polyaniline coated on cellulose sheet by solution plasma process 20 minutes less sediment at the bottom of beaker than of polyaniline coated on cellulose sheet by oxidative polymerization 60 minutes as seen in figure 4.21. Thus, solution plasma process has higher deposition capacity for coating polyaniline on cellulose sheet than oxidative polymerization.

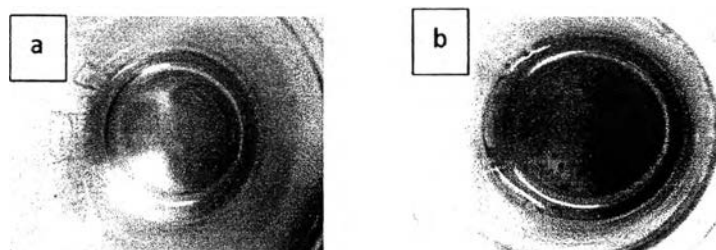


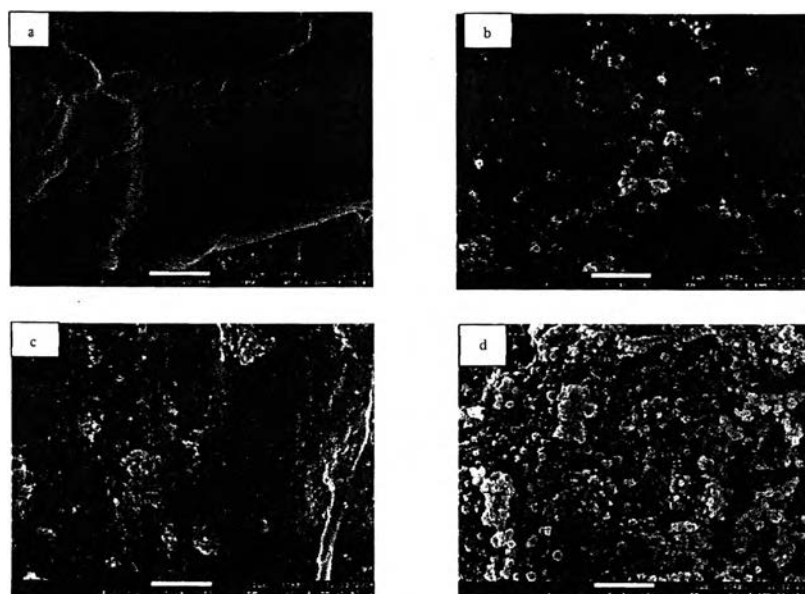
**Figure 4.21** Polyaniline coated on cellulose sheet by a) solution plasma process 20 minutes and b) oxidative polymerization 60 minutes.

#### 4.3.6 Compare Molecular Weight of Polyaniline by Solution Plasma Process and Oxidative Polymerization

The molecular weight of polyaniline by solution plasma process was 20100 Daltons and the molecular weight of polyaniline by oxidative polymerization was 19600 Daltons. The molecular weight of polyaniline by solution plasma process was higher than molecular weight of polyaniline by oxidative polymerization may be due to solution plasma process can help to improve the polymerization efficiency of polyaniline from aniline monomer.

#### 4.3.7 Morphology Analysis

The images of polyaniline coated on plasma treated cellulose sheets by solution plasma were examined by scanning electron microscopy as showed in figure 4.22. Figure 4.22a, shows only the treated cellulose sheet without polyaniline, it was form continuous fibers and smooth surface. In addition, the aniline monomer was added in to the cellulose fibers with different ratios. The weight ratios of cellulose fibers to aniline monomer were 1:0.5, 1:1, 1:5 and 1:6, their surface morphology were showed on figure 4.22. The SEM images reveal that polyaniline on surface of cellulose sheet was increased with increasing the ratio of aniline monomer. However, cellulose to aniline monomer 1:6 the polyaniline on the surface start to agglomerate as seen in the figure 4.22e.



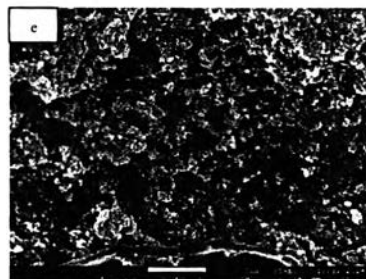


**Figure 4.22** SEM images of polyaniline coated on solution plasma treated cellulose sheets with cellulose to aniline weight ratio a) 1:0, b) 1:0.5, c) 1:1, d) 1:5 and e) 1:6.

#### 4.3.8 Electrical Conductivity

Room temperature DC electrical conductivity values of polyaniline coated on cellulose sheet were measured by two point probe. It found that cellulose fibers to aniline monomer 1: 0.5 provided electrical conductivity  $1.02 \times 10^{-4} \pm 1.68 \times 10^{-5}$  S/cm, cellulose to aniline monomer 1:1 provided electrical conductivity  $3.73 \times 10^{-4} \pm 6.70 \times 10^{-5}$  S/cm, cellulose to aniline monomer 1: 5 provided electrical conductivity  $7.42 \times 10^{-4} \pm 7.77 \times 10^{-5}$  S/cm and cellulose to aniline monomer 1: 6 provided electrical conductivity  $4.89 \times 10^{-4} \pm 7.35 \times 10^{-5}$  S/cm. The electrical conductivity of cellulose fibers to aniline monomer 1:6 lower than electrical conductivity of cellulose fibers to aniline monomer 1:5. This is corresponding to the SEM image (figure 4.22e) that polyaniline of cellulose fibers to aniline monomer 1:6 aggregated and covered some areas on the surface of cellulose sheets.



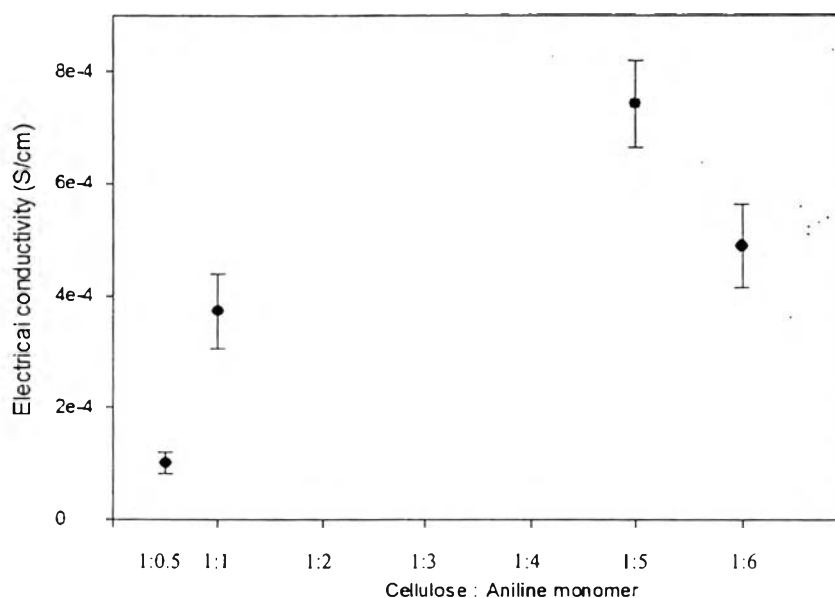


**Figure 4.23** The electrical conductivity of polyaniline coated on cellulose sheets.

#### 4.3.9 Chemical Analysis

The chemical structure of polyaniline coated on cellulose sheet was determined by fourier transform infrared spectroscopy (FTIR). Figure 4.24, it showed both cellulose and polyaniline pattern. The peak of cellulose appeared at wavenumber  $3410\text{ cm}^{-1}$  corresponding to OH-stretching,  $2918\text{ cm}^{-1}$  corresponding to C-H stretching vibration in cellulose and hemicellulose,  $1022\text{ cm}^{-1}$  corresponding to -C-O-C- pyranose ring of cellulose and  $893\text{ cm}^{-1}$  representing  $\beta$ -glycosidic linkages of cellulose. The peak of polyaniline can be observed at wavenumber  $3444\text{ cm}^{-1}$  representing to N-H stretching,  $1590\text{ cm}^{-1}$  representing to N=Q=N (Q is quinoid ring),  $1480\text{ cm}^{-1}$  representing to N=B=N (B is benzene ring) (Elanthikkal S., 2010 and Tariq S., 2014).

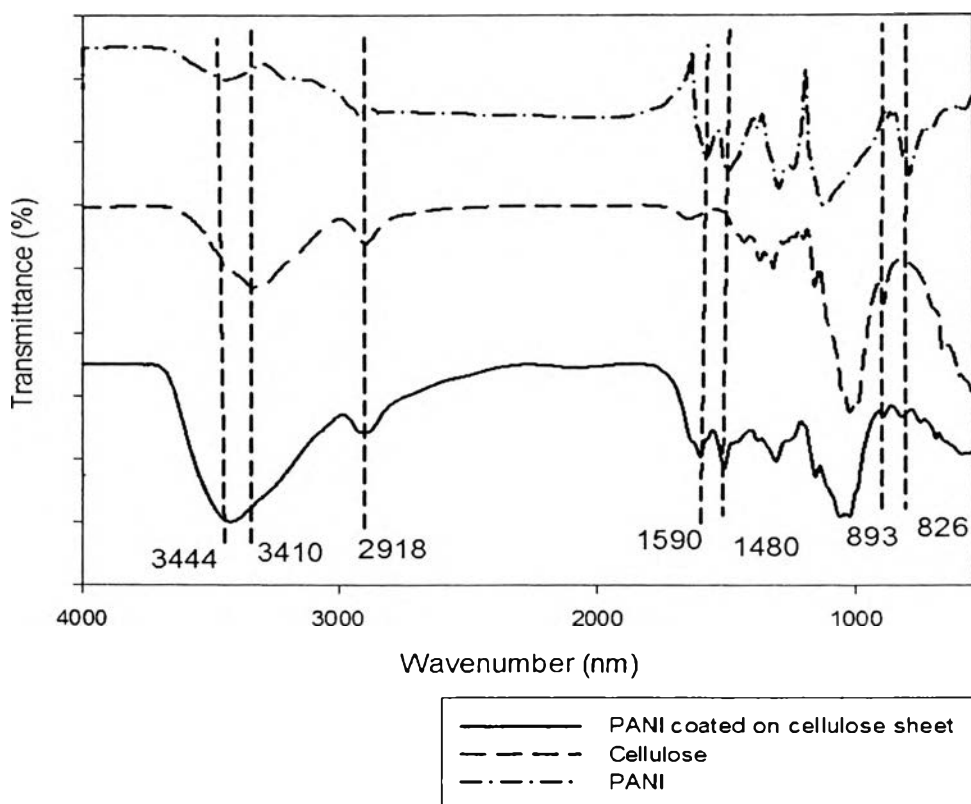


**Figure 4.24** FTIR spectrum of polyaniline coated on cellulose sheet.

#### 4.3.10 Thermogravimetric Analysis

Figure 4.25 showed the TGA thermogram of pure cellulose, pure polyaniline and polyaniline coated on cellulose sheet. For the pure cellulose, graph showed the weight loss in three stages. The first region in the temperature regime of 50-150°C is due to the evaporation of water. The second transition region at around 200-308°C is due to degradation of residual hemicellulose. The third stage of weight loss is occurred about 308°C, is due to the decomposition of cellulose. In comparison, there are three steps of weight loss occurred in TGA thermogram of pure polyaniline. The first steps of weight loss starting at 80-120°C was attributed to the removal of moisture present in the polyaniline. The second step of weight loss occurring in between 120-250°C was due to the evaporation of doping agent (HCl). And the weight loss corresponding to the final step at 450-550°C is mainly attributed to thermal decomposition of polyaniline. For the polyaniline coated on cellulose sheet, also there are three steps of weight loss appeared in TGA thermogram. The

first step of weight loss starting at 80-120°C was due to removal of moisture present in it. The second step of weight loss occurring during 120-308°C, there are two reasons for supporting. The first one is due to the decomposition of residual hemicellulose (that cannot completely remove by treatment process) and another reason is due to the evaporation of doping agent (HCl). In addition, the final step of weight loss at 450-550°C corresponding to thermal decomposition of polyaniline (Wang H., 2012 and Ragupathy S., 2012). The polyaniline coated on cellulose sheet displayed higher amount of residue than pure cellulose, which can be explained in the way that polyaniline coating acted as protective barrier on the surface of cellulose against thermal degradation (Wang H., 2012).

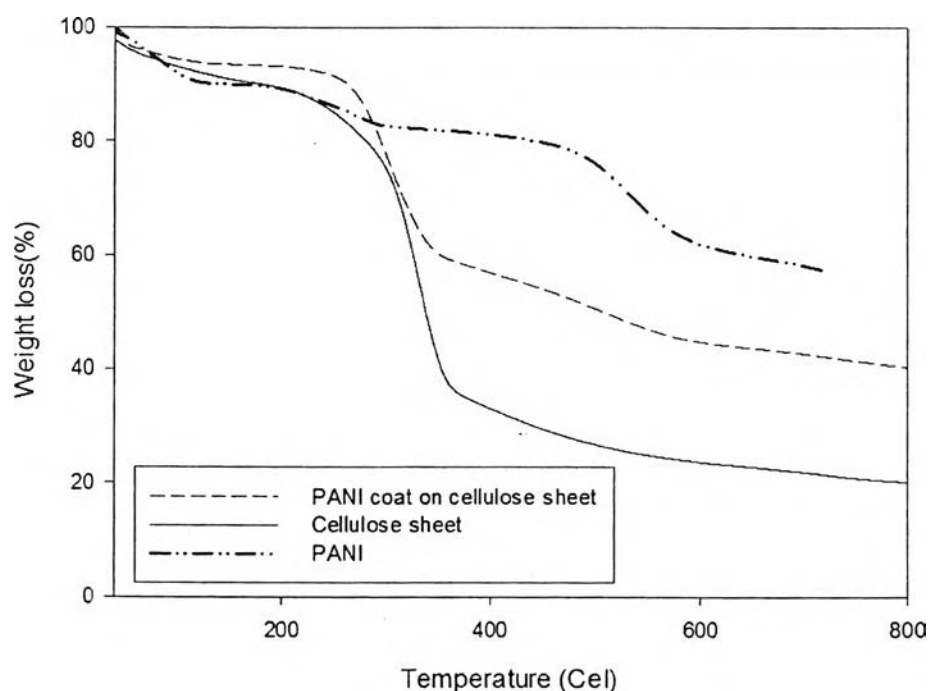


**Figure 4.25** The thermogravimetric analysis of polyaniline coated on cellulose sheet.

#### 4.3.11 The Propose Mechanism of Polyaniline Coated on Cellulose Sheets

In solution plasma process, the water can dissociated to occurred hydroxyl radicals (OH<sup>•</sup>), hydrogen radicals (H<sup>•</sup>) and high energy electrons (Takai O., 2008) as seen in the figure 4.26. In addition, hydroxyl radicals and hydrogen radicals from the dissociation of water by solution plasma can help the reaction of polyaniline

by conventional oxidative polymerization move forward. Because the hydrogen radicals can help hydrochloric acid to change from aniline monomer to anilinium in the first step and hydroxyl radicals can help to abstract the proton ( $H^+$ ) when polymerized polyaniline as showed in the figure 4.27.

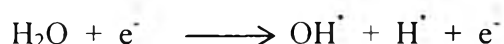


**Figure 4.26** The dissociation of water in solution plasma process.

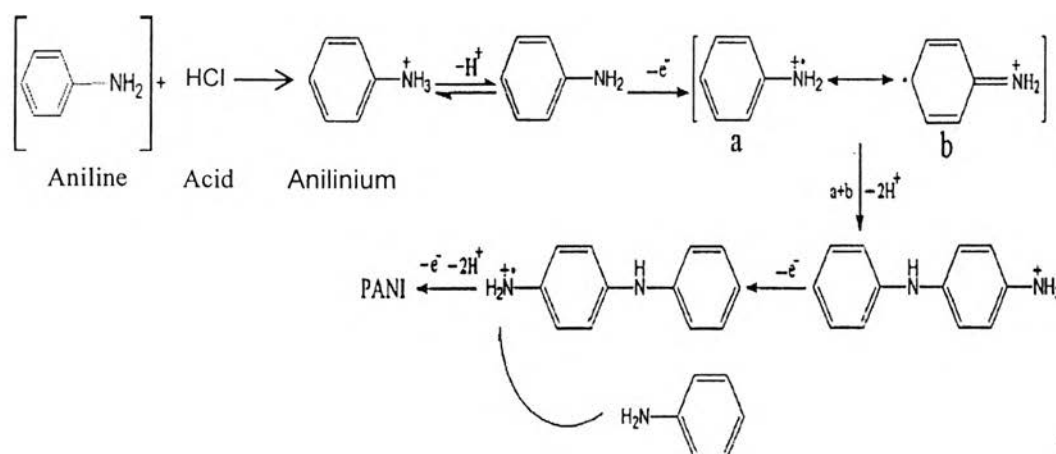


**Figure 4.27** The propose mechanism of polyaniline coated on cellulose sheet.

#### 4.4 Characterization of Polyaniline/Silver Particles Co-Coated Cellulose Sheet

##### 4.4.1 Effect of Ratio between Silver Nitrate and Sodium Borohydride

In this step reducing agent that used for change from silver nitrate to silver particles was sodium borohydride ( $NaBH_4$ ). The ratio of silver nitrate to sodium borohydride was selected by used the ratio that can provided highest silver particles. From figure 4.26 the silver nitrate to sodium borohydride ratio 1:2 can gave the highest amount of silver particles, if the ratio of silver nitrate to sodium borohydride higher than 1:2 there is no effect on amount of silver particles.

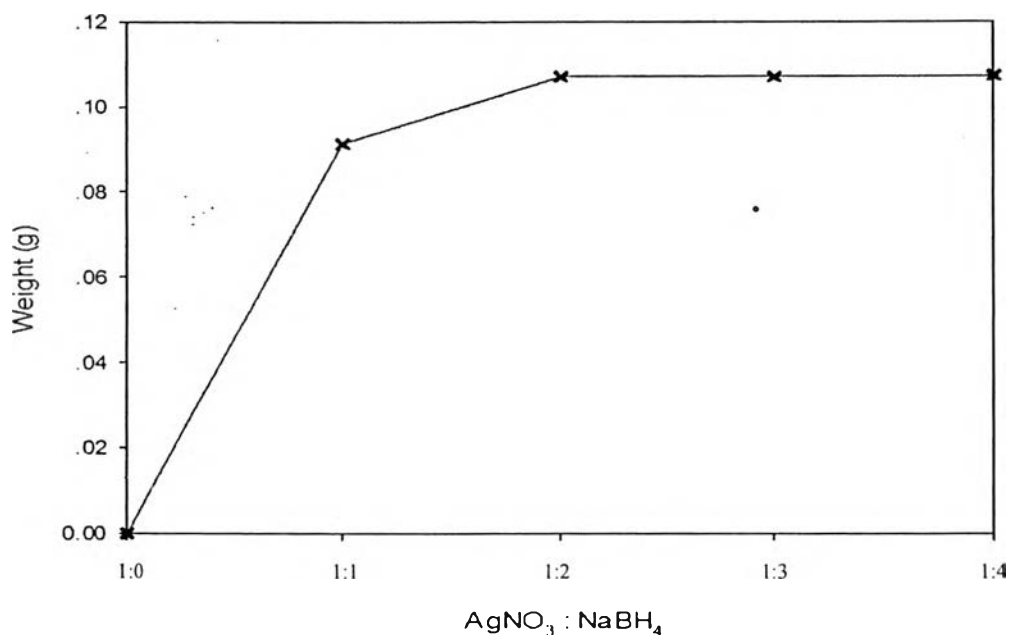


**Figure 4.28** The silver particles weight by using different silver nitrate to reducing agent ratio.

#### 4.4.2 The Morphology and Size of Silver Particles

The TEM image shows the morphology of silver particles which are synthesized from reducing agent and solution plasma. It can be seen from figure 4.27, their shape are spherical. The size of silver particles are various between 1-10 nm and 71-80 nm as seen from figure 4.28. Thus, the average size of silver particles is  $23.9 \pm 14.91$  nm. In addition, the TEM image of silver particles which are synthesized from reducing agent as showed in figure 4.31. The shape is similar with synthesized by reducing agent and solution plasma. The average size of silver particles that synthesized by reducing agent is  $37.4 \pm 94.1$  nm as showed in figure 4.32. The silver particles from solution plasma and reducing agent have size smaller than silver particles from only reducing agent. It can conclude that plasma has effect on the size of silver particles.

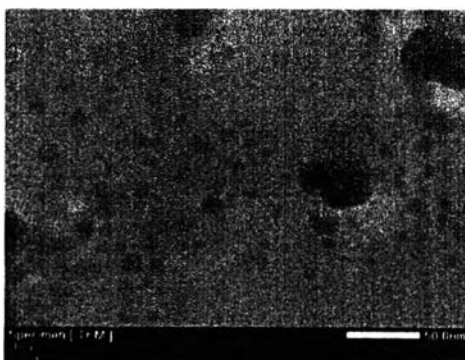


**Figure 4.29** TEM image of silver particles by using reducing agent and solution plasma.

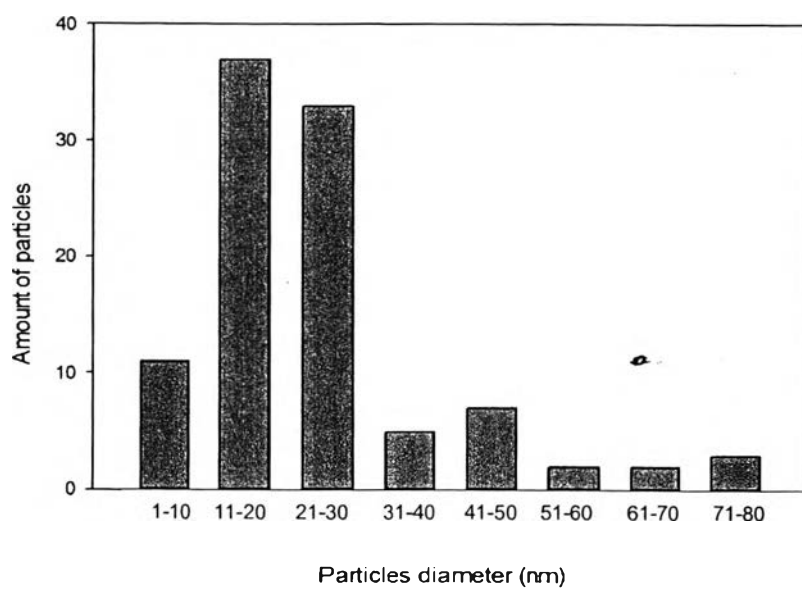


**Figure 4.30** The particles size histogram of silver particles by using reducing agent and solution plasma.

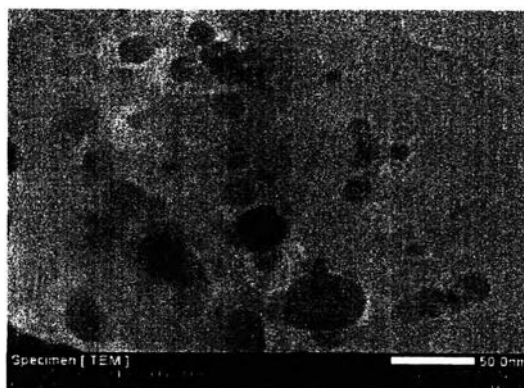


**Figure 4.31** TEM image of silver particles by using reducing agent.

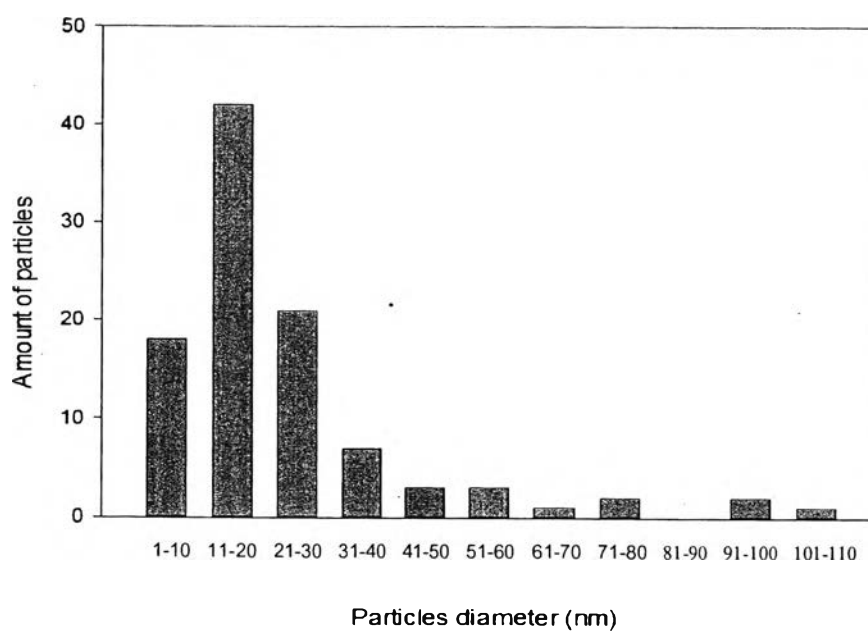


**Figure 4.32** The particles size histogram of silver particles by using reducing agent.

#### 4.4.3 Electrical Conductivity

The polyaniline coated on cellulose sheets were improved the electrical conductivity values by adding silver particles. The different concentrations of silver nitrate were added into polyaniline coated on cellulose sheets. Normally, the electrical conductivity of polyaniline coated on cellulose has electrical conductivity  $7.42 \times 10^{-4} \pm 7.77 \times 10^{-5}$  S/cm. When added silver nitrate concentration 0.1 M, electrical conductivity can increase to  $9.96 \times 10^{-4} \pm 1.08 \times 10^{-4}$  S/cm. Silver nitrate concentration 0.3 M, electrical conductivity can increase to  $1.48 \times 10^{-3} \pm 2.96 \times 10^{-4}$  S/cm. Silver nitrate concentration 0.5 M, electrical conductivity can increase to  $2.62 \times 10^{-3} \pm 2.57 \times 10^{-4}$  S/cm. Silver nitrate concentration 0.7 M, electrical conductivity can increase to  $3.36 \times 10^{-3} \pm 2.02 \times 10^{-4}$  S/cm. The silver nitrate cannot used higher than 0.7 M due to the plasma cannot generate. Therefore, the highest electrical conductivity of polyaniline/silver particles co-coated cellulose sheet is  $3.36 \times 10^{-3}$  S/cm with silver nitrate concentration 0.7 M as seen in the figure 4.29. When silver concentration increased, the electrical conductivity also increased could be due to decreasing inter-particles distance between Ag-Ag particles.

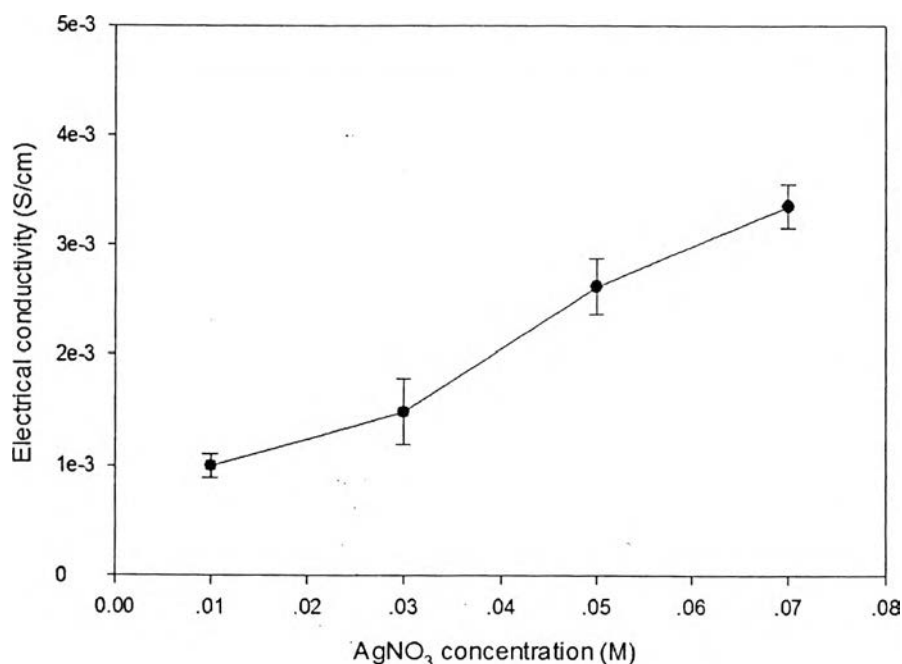


**Figure 4.33** The electrical conductivity of polyaniline/silver particles co-coated cellulose sheet.